

Nuclear Modification of ψ' , χ_c and J/ψ Production in $d+\text{Au}$ Collisions at $\sqrt{s_{NN}} = 200 \text{ GeV}$

A. Adare,¹³ C. Aidala,^{41,42} N.N. Ajitanand,⁵⁸ Y. Akiba,^{54,55} H. Al-Bataineh,⁴⁸ J. Alexander,⁵⁸ A. Angerami,¹⁴
K. Aoki,^{33,54} N. Apadula,⁵⁹ Y. Aramaki,^{12,54} E.T. Atomssa,³⁴ R. Averbeck,⁵⁹ T.C. Awes,⁵⁰ B. Azmoun,⁷
V. Babintsev,²³ M. Bai,⁶ G. Baksay,¹⁹ L. Baksay,¹⁹ K.N. Barish,⁸ B. Bassalleck,⁴⁷ A.T. Basye,¹ S. Bathe,^{5,8,55}
V. Baublis,⁵³ C. Baumann,⁴³ A. Bazilevsky,⁷ S. Belikov,^{7,*} R. Belmont,⁶³ R. Bennett,⁵⁹ J.H. Bhom,⁶⁷ D.S. Blau,³²
J.S. Bok,⁶⁷ K. Boyle,⁵⁹ M.L. Brooks,³⁷ H. Buesching,⁷ V. Bumazhnov,²³ G. Bunce,^{7,55} S. Butsyk,³⁷ S. Campbell,⁵⁹
A. Caringi,⁴⁴ C.-H. Chen,⁵⁹ C.Y. Chi,¹⁴ M. Chiu,⁷ I.J. Choi,⁶⁷ J.B. Choi,¹⁰ R.K. Choudhury,⁴ P. Christiansen,³⁹
T. Chujo,⁶² P. Chung,⁵⁸ O. Chvala,⁸ V. Cianciolo,⁵⁰ Z. Citron,⁵⁹ B.A. Cole,¹⁴ Z. Conesa del Valle,³⁴ M. Connors,⁵⁹
M. Csanád,¹⁷ T. Csörgő,⁶⁶ T. Dahms,⁵⁹ S. Dairaku,^{33,54} I. Danchev,⁶³ K. Das,²⁰ A. Datta,⁴¹ G. David,⁷
M.K. Dayananda,²¹ A. Denisov,²³ A. Deshpande,^{55,59} E.J. Desmond,⁷ K.V. Dharmawardane,⁴⁸ O. Dietzsch,⁵⁷
A. Dion,^{27,59} M. Donadelli,⁵⁷ O. Drapier,³⁴ A. Drees,⁵⁹ K.A. Drees,⁶ J.M. Durham,^{37,59} A. Durum,²³ D. Dutta,⁴
L. D'Orazio,⁴⁰ S. Edwards,²⁰ Y.V. Efremenko,⁵⁰ F. Ellinghaus,¹³ T. Engelmores,¹⁴ A. Enokizono,⁵⁰ H. En'yo,^{54,55}
S. Esumi,⁶² B. Fadern,⁴⁴ D.E. Fields,⁴⁷ M. Finger,⁹ M. Finger, Jr.,⁹ F. Fleuret,³⁴ S.L. Fokin,³² Z. Fraenkel,^{65,*}
J.E. Frantz,^{49,59} A. Franz,⁷ A.D. Frawley,²⁰ K. Fujiwara,⁵⁴ Y. Fukao,⁵⁴ T. Fusayasu,⁴⁶ I. Garishvili,⁶⁰ A. Glenn,³⁶
H. Gong,⁵⁹ M. Gonin,³⁴ Y. Goto,^{54,55} R. Granier de Cassagnac,³⁴ N. Grau,^{2,14} S.V. Greene,⁶³ G. Grim,³⁷
M. Grosse Perdekamp,²⁴ T. Gunji,¹² H.-Å. Gustafsson,^{39,*} J.S. Haggerty,⁷ K.I. Hahn,¹⁸ H. Hamagaki,¹²
J. Hamblen,⁶⁰ R. Han,⁵² J. Hanks,¹⁴ E. Haslum,³⁹ R. Hayano,¹² X. He,²¹ M. Heffner,³⁶ T.K. Hemmick,⁵⁹
T. Hester,⁸ J.C. Hill,²⁷ M. Hohlmann,¹⁹ W. Holzmann,¹⁴ K. Homma,²² B. Hong,³¹ T. Horaguchi,²² D. Hornback,⁶⁰
S. Huang,⁶³ T. Ichihara,^{54,55} R. Ichimiya,⁵⁴ Y. Ikeda,⁶² K. Imai,^{28,33,54} M. Inaba,⁶² D. Isenhower,¹
M. Ishihara,⁵⁴ M. Issah,⁶³ D. Ivanishev,⁵³ Y. Iwanaga,²² B.V. Jacak,⁵⁹ J. Jia,^{7,58} X. Jiang,³⁷ J. Jin,¹⁴
B.M. Johnson,⁷ T. Jones,¹ K.S. Joo,⁴⁵ D. Jouan,⁵¹ D.S. Jumper,¹ F. Kajihara,¹² J. Kamin,⁵⁹ J.H. Kang,⁶⁷
J. Kapustinsky,³⁷ K. Karatsu,^{33,54} M. Kasai,^{54,56} D. Kawall,^{41,55} M. Kawashima,^{54,56} A.V. Kazantsev,³²
T. Kempel,²⁷ A. Khanzadeev,⁵³ K.M. Kijima,²² J. Kikuchi,⁶⁴ A. Kim,¹⁸ B.I. Kim,³¹ D.J. Kim,²⁹ E.-J. Kim,¹⁰
Y.-J. Kim,²⁴ E. Kinney,¹³ Á. Kiss,¹⁷ E. Kistenev,⁷ D. Kleinjan,⁸ L. Kochenda,⁵³ B. Komkov,⁵³ M. Konno,⁶²
J. Koster,²⁴ A. Král,¹⁵ A. Kravitz,¹⁴ G.J. Kunde,³⁷ K. Kurita,^{54,56} M. Kurosawa,⁵⁴ Y. Kwon,⁶⁷ G.S. Kyle,⁴⁸
R. Lacey,⁵⁸ Y.S. Lai,¹⁴ J.G. Lajoie,²⁷ A. Lebedev,²⁷ D.M. Lee,³⁷ J. Lee,¹⁸ K.B. Lee,³¹ K.S. Lee,³¹
M.J. Leitch,³⁷ M.A.L. Leite,⁵⁷ X. Li,¹¹ P. Lichtenwalner,⁴⁴ P. Liebing,⁵⁵ L.A. Linden Levy,¹³ T. Liška,¹⁵
H. Liu,³⁷ M.X. Liu,³⁷ B. Love,⁶³ D. Lynch,⁷ C.F. Maguire,⁶³ Y.I. Makdisi,⁶ M.D. Malik,⁴⁷ V.I. Manko,³²
E. Mannel,¹⁴ Y. Mao,^{52,54} H. Masui,⁶² F. Matathias,¹⁴ M. McCumber,⁵⁹ P.L. McGaughey,³⁷ D. McGlinchey,^{13,20}
N. Means,⁵⁹ B. Meredith,²⁴ Y. Miake,⁶² T. Mibe,³⁰ A.C. Mignerey,⁴⁰ K. Miki,^{54,62} A. Milov,⁷ J.T. Mitchell,⁷
A.K. Mohanty,⁴ H.J. Moon,⁴⁵ Y. Morino,¹² A. Morreale,⁸ D.P. Morrison,^{7,†} T.V. Moukhanova,³² T. Murakami,³³
J. Murata,^{54,56} S. Nagamiya,³⁰ J.L. Nagle,^{13,‡} M. Naglis,⁶⁵ M.I. Nagy,⁶⁶ I. Nakagawa,^{54,55} Y. Nakamiya,²²
K.R. Nakamura,^{33,54} T. Nakamura,⁵⁴ K. Nakano,⁵⁴ S. Nam,¹⁸ J. Newby,³⁶ M. Nguyen,⁵⁹ M. Nihashi,²² R. Nouicer,⁷
A.S. Nyanin,³² C. Oakley,²¹ E. O'Brien,⁷ S.X. Oda,¹² C.A. Ogilvie,²⁷ M. Oka,⁶² K. Okada,⁵⁵ Y. Onuki,⁵⁴
A. Oskarsson,³⁹ M. Ouchida,^{22,54} K. Ozawa,¹² R. Pak,⁷ V. Pantuev,^{25,59} V. Papavassiliou,⁴⁸ I.H. Park,¹⁸
S.K. Park,³¹ W.J. Park,³¹ S.F. Pate,⁴⁸ H. Pei,²⁷ J.-C. Peng,²⁴ H. Pereira,¹⁶ D. Perepelitsa,¹⁴ D.Yu. Peressounko,³²
R. Petti,⁵⁹ C. Pinkenburg,⁷ R.P. Pisani,⁷ M. Proissl,⁵⁹ M.L. Purschke,⁷ H. Qu,²¹ J. Rak,²⁹ I. Ravinovich,⁶⁵
K.F. Read,^{50,60} S. Rembeczki,¹⁹ K. Reygers,⁴³ V. Riabov,⁵³ Y. Riabov,⁵³ E. Richardson,⁴⁰ D. Roach,⁶³
G. Roche,³⁸ S.D. Rolnick,⁸ M. Rosati,²⁷ C.A. Rosen,¹³ S.S.E. Rosendahl,³⁹ P. Ružička,²⁶ B. Sahlmueller,^{43,59}
N. Saito,³⁰ T. Sakaguchi,⁷ K. Sakashita,^{54,61} V. Samsonov,⁵³ S. Sano,^{12,64} T. Sato,⁶² S. Sawada,³⁰ K. Sedgwick,⁸
J. Seele,¹³ R. Seidl,^{24,55} R. Seto,⁸ D. Sharma,⁶⁵ I. Shein,²³ T.-A. Shibata,^{54,61} K. Shigaki,²² M. Shimomura,⁶²
K. Shoji,^{33,54} P. Shukla,⁴ A. Sickles,⁷ C.L. Silva,²⁷ D. Silvermyr,⁵⁰ C. Silvestre,¹⁶ K.S. Sim,³¹ B.K. Singh,³
C.P. Singh,³ V. Singh,³ M. Slunečka,⁹ R.A. Soltz,³⁶ W.E. Sondheim,³⁷ S.P. Sorensen,⁶⁰ I.V. Sourikova,⁷
P.W. Stankus,⁵⁰ E. Stenlund,³⁹ S.P. Stoll,⁷ T. Sugitate,²² A. Sukhanov,⁷ J. Sziklai,⁶⁶ E.M. Takagui,⁵⁷
A. Taketani,^{54,55} R. Tanabe,⁶² Y. Tanaka,⁴⁶ S. Taneja,⁵⁹ K. Tanida,^{33,54,55} M.J. Tannenbaum,⁷ S. Tarafdar,³
A. Taranenko,⁵⁸ H. Themann,⁵⁹ D. Thomas,¹ T.L. Thomas,⁴⁷ M. Togawa,⁵⁵ A. Toia,⁵⁹ L. Tomášek,²⁶ H. Torii,²²
R.S. Towell,¹ I. Tserruya,⁶⁵ Y. Tsuchimoto,²² C. Vale,⁷ H. Valle,⁶³ H.W. van Hecke,³⁷ E. Vazquez-Zambrano,¹⁴
A. Veicht,²⁴ J. Velkovska,⁶³ R. Vértesi,⁶⁶ M. Virius,¹⁵ V. Vrba,²⁶ E. Vznuzdaev,⁵³ X.R. Wang,⁴⁸ D. Watanabe,²²
K. Watanabe,⁶² Y. Watanabe,^{54,55} F. Wei,²⁷ R. Wei,⁵⁸ J. Wessels,⁴³ S.N. White,⁷ D. Winter,¹⁴ C.L. Woody,⁷

R.M. Wright,¹ M. Wysocki,¹³ Y.L. Yamaguchi,¹² K. Yamaura,²² R. Yang,²⁴ A. Yanovich,²³ J. Ying,²¹
S. Yokkaichi,^{54,55} Z. You,⁵² G.R. Young,⁵⁰ I. Younus,^{35,47} I.E. Yushmanov,³² W.A. Zajc,¹⁴ and S. Zhou¹¹

(PHENIX Collaboration)

- ¹Abilene Christian University, Abilene, Texas 79699, USA
²Department of Physics, Augustana College, Sioux Falls, South Dakota 57197, USA
³Department of Physics, Banaras Hindu University, Varanasi 221005, India
⁴Bhabha Atomic Research Centre, Bombay 400 085, India
⁵Baruch College, City University of New York, New York, New York, 10010 USA
⁶Collider-Accelerator Department, Brookhaven National Laboratory, Upton, New York 11973-5000, USA
⁷Physics Department, Brookhaven National Laboratory, Upton, New York 11973-5000, USA
⁸University of California - Riverside, Riverside, California 92521, USA
⁹Charles University, Ovocný trh 5, Praha 1, 116 36, Prague, Czech Republic
¹⁰Chonbuk National University, Jeonju, 561-756, Korea
¹¹Science and Technology on Nuclear Data Laboratory, China Institute of Atomic Energy, Beijing 102413, P. R. China
¹²Center for Nuclear Study, Graduate School of Science, University of Tokyo, 7-3-1 Hongo, Bunkyo, Tokyo 113-0033, Japan
¹³University of Colorado, Boulder, Colorado 80309, USA
¹⁴Columbia University, New York, New York 10027 and Nevis Laboratories, Irvington, New York 10533, USA
¹⁵Czech Technical University, Zikova 4, 166 36 Prague 6, Czech Republic
¹⁶Dapnia, CEA Saclay, F-91191, Gif-sur-Yvette, France
¹⁷ELTE, Eötvös Loránd University, H - 1117 Budapest, Pázmány P. s. 1/A, Hungary
¹⁸Ewha Womans University, Seoul 120-750, Korea
¹⁹Florida Institute of Technology, Melbourne, Florida 32901, USA
²⁰Florida State University, Tallahassee, Florida 32306, USA
²¹Georgia State University, Atlanta, Georgia 30303, USA
²²Hiroshima University, Kagamiyama, Higashi-Hiroshima 739-8526, Japan
²³IHEP Protvino, State Research Center of Russian Federation, Institute for High Energy Physics, Protvino, 142281, Russia
²⁴University of Illinois at Urbana-Champaign, Urbana, Illinois 61801, USA
²⁵Institute for Nuclear Research of the Russian Academy of Sciences, prospekt 60-letiya Oktyabrya 7a, Moscow 117312, Russia
²⁶Institute of Physics, Academy of Sciences of the Czech Republic, Na Slovance 2, 182 21 Prague 8, Czech Republic
²⁷Iowa State University, Ames, Iowa 50011, USA
²⁸Advanced Science Research Center, Japan Atomic Energy Agency, 2-4
Shirakata Shirane, Tokai-mura, Naka-gun, Ibaraki-ken 319-1195, Japan
²⁹Helsinki Institute of Physics and University of Jyväskylä, P.O.Box 35, FI-40014 Jyväskylä, Finland
³⁰KEK, High Energy Accelerator Research Organization, Tsukuba, Ibaraki 305-0801, Japan
³¹Korea University, Seoul, 136-701, Korea
³²Russian Research Center "Kurchatov Institute", Moscow, 123098 Russia
³³Kyoto University, Kyoto 606-8502, Japan
³⁴Laboratoire Leprince-Ringuet, Ecole Polytechnique, CNRS-IN2P3, Route de Saclay, F-91128, Palaiseau, France
³⁵Physics Department, Lahore University of Management Sciences, Lahore, Pakistan
³⁶Lawrence Livermore National Laboratory, Livermore, California 94550, USA
³⁷Los Alamos National Laboratory, Los Alamos, New Mexico 87545, USA
³⁸LPC, Université Blaise Pascal, CNRS-IN2P3, Clermont-Fd, 63177 Aubiere Cedex, France
³⁹Department of Physics, Lund University, Box 118, SE-221 00 Lund, Sweden
⁴⁰University of Maryland, College Park, Maryland 20742, USA
⁴¹Department of Physics, University of Massachusetts, Amherst, Massachusetts 01003-9337, USA
⁴²Department of Physics, University of Michigan, Ann Arbor, Michigan 48109-1040, USA
⁴³Institut für Kernphysik, University of Muenster, D-48149 Muenster, Germany
⁴⁴Muhlenberg College, Allentown, Pennsylvania 18104-5586, USA
⁴⁵Myongji University, Yongin, Kyonggido 449-728, Korea
⁴⁶Nagasaki Institute of Applied Science, Nagasaki-shi, Nagasaki 851-0193, Japan
⁴⁷University of New Mexico, Albuquerque, New Mexico 87131, USA
⁴⁸New Mexico State University, Las Cruces, New Mexico 88003, USA
⁴⁹Department of Physics and Astronomy, Ohio University, Athens, Ohio 45701, USA
⁵⁰Oak Ridge National Laboratory, Oak Ridge, Tennessee 37831, USA
⁵¹IPN-Orsay, Université Paris Sud, CNRS-IN2P3, BP1, F-91406, Orsay, France
⁵²Peking University, Beijing 100871, P. R. China
⁵³PNPI, Petersburg Nuclear Physics Institute, Gatchina, Leningrad region, 188300, Russia
⁵⁴RIKEN Nishina Center for Accelerator-Based Science, Wako, Saitama 351-0198, Japan
⁵⁵RIKEN BNL Research Center, Brookhaven National Laboratory, Upton, New York 11973-5000, USA
⁵⁶Physics Department, Rikkyo University, 3-34-1 Nishi-Ikebukuro, Toshima, Tokyo 171-8501, Japan
⁵⁷Universidade de São Paulo, Instituto de Física, Caixa Postal 66318, São Paulo CEP05315-970, Brazil
⁵⁸Chemistry Department, Stony Brook University, SUNY, Stony Brook, New York 11794-3400, USA
⁵⁹Department of Physics and Astronomy, Stony Brook University, SUNY, Stony Brook, New York 11794-3400, USA

⁶⁰University of Tennessee, Knoxville, Tennessee 37996, USA

⁶¹Department of Physics, Tokyo Institute of Technology, Oh-okayama, Meguro, Tokyo 152-8551, Japan

⁶²Institute of Physics, University of Tsukuba, Tsukuba, Ibaraki 305, Japan

⁶³Vanderbilt University, Nashville, Tennessee 37235, USA

⁶⁴Waseda University, Advanced Research Institute for Science and Engineering, 17 Kikui-cho, Shinjuku-ku, Tokyo 162-0044, Japan

⁶⁵Weizmann Institute, Rehovot 76100, Israel

⁶⁶Institute for Particle and Nuclear Physics, Wigner Research Centre for Physics, Hungarian Academy of Sciences (Wigner RCP, RMKI) H-1525 Budapest 114, POBox 49, Budapest, Hungary

⁶⁷Yonsei University, IPAP, Seoul 120-749, Korea

(Dated: August 14, 2019)

We present results for three charmonia states (ψ' , χ_c , and J/ψ) in d +Au collisions at $|y| < 0.35$ and $\sqrt{s_{NN}} = 200$ GeV. We find that the modification of the ψ' yield relative to that of the J/ψ scales approximately with charged particle multiplicity at midrapidity across p +A, d +Au, and A +A results from the Super Proton Synchrotron and the Relativistic Heavy Ion Collider. In large-impact-parameter collisions we observe a similar suppression for the ψ' and J/ψ , while in small-impact-parameter collisions the more weakly bound ψ' is more strongly suppressed. Owing to the short time spent traversing the Au nucleus, the larger ψ' suppression in central events is not explained by an increase of the nuclear absorption due to meson formation time effects.

PACS numbers: 25.75.Dw

Understanding the evolution of heavy quark-antiquark pairs into bound color singlet quarkonium states represents a challenge within QCD. An excellent tool for probing the time scale for this evolution is the measurement of production rates for multiple quarkonium states, with different physical sizes and binding energies, in proton (or deuteron) - nucleus collisions. The evolving quark-antiquark pair must traverse the target nucleus, and by varying the path length in the nucleus one can probe this time scale.

Measurements of J/ψ and ψ' production rates at $\sqrt{s_{NN}} = 38.7$ GeV, as a function of Feynman- x (x_F), in proton-nucleus collisions by E866/NuSea [1] show a greater suppression of ψ' production compared to J/ψ production near $x_F \approx 0$, and a comparable suppression for $x_F > 0$. Similar measurements by NA50 [2] at $\sqrt{s_{NN}} = 27.4$ GeV and $x_F \approx 0$ show a stronger suppression of ψ' production, compared to J/ψ production, for larger nuclei. This has been interpreted as an effect of the charmonia formation time [3]. When the time spent traversing the nucleus by the $c\bar{c}$ pair becomes longer than the charmonia formation time, the larger ψ' meson will be further suppressed by a larger nuclear breakup effect. It is critical to test these assumptions at the collision energies provided by the Relativistic Heavy Ion Collider (RHIC), where the time spent traversing the nucleus is expected to be much shorter than this formation time. Also, the binding energy of the ψ' (≈ 0.05 GeV) is significantly smaller than that of the χ_c (≈ 0.20 GeV) or J/ψ (≈ 0.64 GeV) [4], and may play an important role in understanding the effects of producing quarkonia in a nuclear target.

The PHENIX experiment has previously reported measurements of J/ψ production rates in d +Au collisions at $\sqrt{s_{NN}} = 200$ GeV using data collected in 2008 [5, 6].

Here we present measurements of ψ' production rates, as well as the fraction of J/ψ yield which comes from χ_c decays, in d +Au collisions at midrapidity from the same data set. Using the corresponding measurements in p + p collisions by PHENIX [7], we construct the nuclear modification factor, R_{dAu} , for ψ' and χ_c production and compare it with the measurements of the J/ψ R_{dAu} at the same energy.

The PHENIX detector is described in detail in Ref. [8]. The data presented here were collected using the two PHENIX central arms, each of which detect electrons, photons, and hadrons over $|\eta| < 0.35$ and $\Delta\phi = \frac{\pi}{2}$. The d +Au data used in this analysis were recorded using a minimum bias (MB) trigger in coincidence with an additional electron Level-1 trigger. The MB trigger requires at least one hit in each of the two beam-beam counters (BBCs) covering $3 < |\eta| < 3.9$. This MB selection covers $88 \pm 4\%$ of the total d +Au inelastic cross section of 2.26 barns [9]. The electron trigger requires a minimum energy deposited in any group of 2×2 towers in the Electromagnetic Calorimeter and an associated hit in the Ring Imaging Čerenkov counter. Thresholds of 600 and 800 MeV were used, each for roughly half of the data sample. The data set represents analyzed integrated luminosities of 62.7 and 66.2 nb^{-1} for the ψ' and χ_c analyses respectively.

The ψ' invariant yield is calculated as

$$B_{ee} \frac{dN_{\psi'}}{dy} = \frac{cN_{\psi'}}{N_{\text{MB}} \epsilon A \Delta y}, \quad (1)$$

where B_{ee} is the $\psi' \rightarrow e^+e^-$ branching ratio, $N_{\psi'}$ is the measured $\psi' \rightarrow e^+e^-$ yield, N_{MB} is the number of sampled MB events, and Δy is the width of the rapidity bin. A GEANT-3 based model of the PHENIX detector combined with measurements of the momentum dependence

of the single electron trigger efficiency, as described in Ref. [6], is used to calculate the product of the acceptance and efficiency, ϵA , which includes the Level-1 trigger efficiency. This model is also used to estimate the detector effects on the simulated signal and background line shapes when fitting the measured dielectron signal. Following the procedures described in Ref. [6], ϵA is found to have an average value of 0.91% with a relative systematic uncertainty of 6.4%. The correction factor c accounts for the trigger and centrality bias present in events which contain a hard scattering [6]. The track multiplicity dependence of the reconstruction efficiency is negligible in $d+Au$ collisions, and a 1% systematic uncertainty was assigned based on the J/ψ studies performed in Ref. [6].

The $\psi' \rightarrow e^+e^-$ yield is extracted from fits to the unlike-sign (e^+e^-) invariant mass distribution, after the subtraction of the like-sign ($e^+e^+ + e^-e^-$) background, where at least one of the electrons fired the Level-1 trigger. The fit is performed over the mass range $2.0 < M_{ee} [\text{GeV}/c^2] < 5.5$, and includes line shapes for $J/\psi \rightarrow e^+e^-$ and $\psi' \rightarrow e^+e^-$ decays, as well as the remaining correlated background from open heavy flavor and Drell-Yan decays.

The J/ψ and ψ' line shapes include the natural line shape, smeared based on the PHENIX mass resolution, and radiative decays ($J/\psi \rightarrow e^+e^-\gamma$ for $E_\gamma > 100$ MeV), using calculations of the mass distribution from QED [10]. The line shape for Drell-Yan decays was generated using PYTHIA-6 [11]. Line shapes for open heavy flavor decays were generated using three different MC generators, including PYTHIA-6 in both hard scattering and forced charm (or bottom) production modes as well as the MC@NLO generator [12].

After applying the detector acceptance and efficiency effects, the line shapes are fit to the invariant mass distributions. It was found that the heavy flavor line shapes generated using PYTHIA-6 set to hard scattering mode gave the lowest χ^2 per degree of freedom (68.5/68), while those generated using PYTHIA-6 set to charm(bottom) production as well as those generated using MC@NLO provided slightly poorer agreements with a χ^2 per degree of freedom of 79.1/68 and 83.4/68 respectively. The different line shapes resulted in changes in the extracted ψ' yield of less than 20% in peripheral events. In central events there is a very small signal which varies by up to 83% within the different assumed shapes. In all cases, the continuum line shapes were generated for $p+p$ collisions, and may be modified in $d+Au$ collisions. The effect of nuclear shadowing on the Drell-Yan and open heavy flavor line shapes using the EPS09s parametrization [13] was found to change the extracted ψ' yield by less than 5%.

Figure 1 shows the results of the fit for central and peripheral $d+Au$ collisions. The shaded bands represent the combined uncertainty in the fit normalizations, as well as changes in the shape of the correlated background ob-

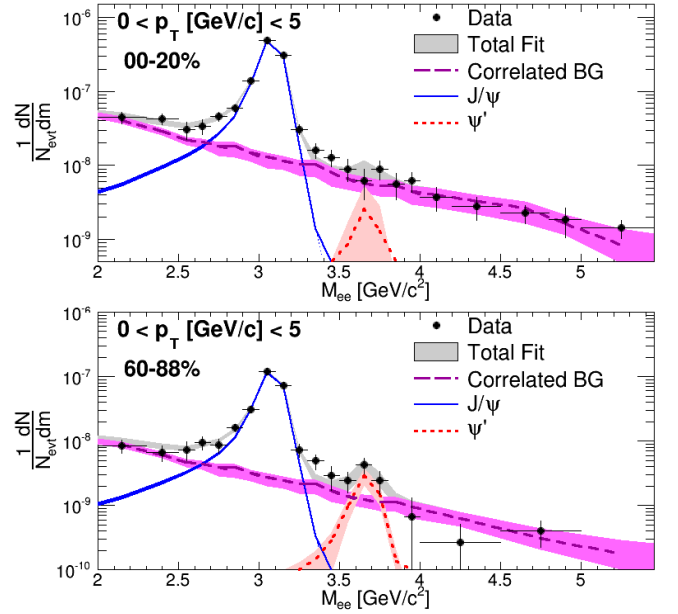


FIG. 1: (Color online) The e^+e^- mass distribution, after like-sign subtraction, for 0–20% (Top) and 60–88% (Bottom) $d+Au$ collisions. The line shapes are those fit to the data in order to extract the ψ' yield.

tained using the three different sets of open heavy flavor line shapes.

The resulting invariant yields are used, in conjunction with the measured values in $p+p$ collisions [7], to calculate the nuclear modification factor, R_{dAu} . The ψ' R_{dAu} is calculated as

$$R_{dAu}^{\psi'} = \frac{dN_{\psi'}^{dAu}/dy}{N_{\text{coll}} dN_{\psi'}^{pp}/dy}, \quad (2)$$

where N_{coll} is the mean number of nucleon-nucleon collisions, and $dN_{\psi'}^{dAu}/dy$ and $dN_{\psi'}^{pp}/dy$ are the measured invariant yields in $d+Au$ and $p+p$ collisions, respectively. The value of N_{coll} is calculated using a Glauber Monte Carlo model coupled with a simulation of the PHENIX BBC response (see [6] for details). We find a value for the ψ' nuclear modification factor of $R_{dAu}^{\psi'} = 0.54 \pm 0.11(\text{stat})_{-0.16}^{+0.19}(\text{syst})$ in 0–100% centrality integrated $d+Au$ collisions.

The feed-down fraction of the inclusive J/ψ yield from χ_c decays in $d+Au$ collisions ($F_{\chi_c \rightarrow J/\psi}^{dAu}$) is measured via the $\chi_c \rightarrow J/\psi + \gamma \rightarrow e^+e^- + \gamma$ decay channel, where the $e^+e^- \gamma$ is fully reconstructed in the PHENIX central arms. The procedure for extracting $F_{\chi_c \rightarrow J/\psi}^{dAu}$ is the same as that presented for $p+p$ collisions in [7] for a data sample of comparable statistical precision. The final feed-down fraction is found to be $F_{\chi_c \rightarrow J/\psi}^{dAu} = 0.32 \pm 0.09(\text{stat}) \pm 0.03(\text{syst})$.

Using the measured feed-down fraction in $p+p$ colli-

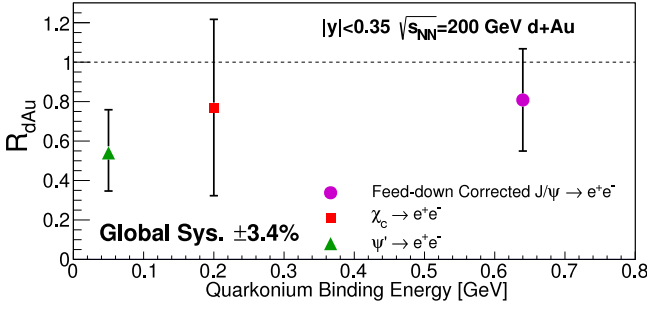


FIG. 2: (Color online) The ψ' , χ_c , and J/ψ R_{dAu} for 0–100% centrality integrated $d+Au$ collisions as a function of the quarkonia binding energy, where the J/ψ R_{dAu} has been corrected for the effects of ψ' and χ_c feed-down. The systematic uncertainties which are not correlated between the three points and have been added in quadrature with the statistical uncertainties for plotting. The common global scale uncertainty is quoted on the plot. The binding energies are the differences between the quarkonium masses and the open charm threshold, and are taken from Ref. [4].

sions and the J/ψ R_{dAu} , the χ_c R_{dAu} is calculated as

$$R_{dAu}^{\chi_c} = R_{dAu}^{J/\psi} \times \frac{F_{\chi_c \rightarrow J/\psi}^{dAu}}{F_{\chi_c \rightarrow J/\psi}^{pp}}. \quad (3)$$

The nuclear modification of χ_c production in $d+Au$ collisions is found to be $R_{dAu}^{\chi_c} = 0.77 \pm 0.41(\text{stat}) \pm 0.18(\text{syst})$.

With the ψ' and χ_c nuclear modification in hand, it is possible to correct the measured modification of inclusive J/ψ production for their feed-down effects, thus giving a closer representation of the modification of direct J/ψ production. Here we use the ψ' and χ_c feed-down fractions in $p+p$ collisions measured by PHENIX in Ref. [7]. The corrected J/ψ modification is calculated as

$$R_{dAu}^{\text{direct } J/\psi} = \frac{(R_{dAu}^{\text{incl } J/\psi} - F_{\psi' \rightarrow J/\psi}^{pp} R_{dAu}^{\psi'} - F_{\chi_c \rightarrow J/\psi}^{pp} R_{dAu}^{\chi_c})}{(1 - F_{\psi' \rightarrow J/\psi}^{pp} - F_{\chi_c \rightarrow J/\psi}^{pp})}, \quad (4)$$

where $R_{dAu}^{\text{incl } J/\psi} = 0.77 \pm 0.02(\text{stat}) \pm 0.16(\text{syst})$ is the modification of inclusive J/ψ production, reported in Ref. [5]. This gives a feed-down corrected J/ψ modification of $R_{dAu}^{\text{direct } J/\psi} = 0.81 \pm 0.12(\text{stat}) \pm 0.23(\text{syst})$. While there still remains a contribution from $B \rightarrow J/\psi + X$ decays, its value is expected to be small ($\approx 2.7\%$ [14]).

Figure 2 plots the nuclear modification as a function of the quarkonia binding energy. The χ_c measurement has large statistical and systematic uncertainties, but the J/ψ and ψ' modifications suggest that there is a decrease in suppression with increasing binding energy.

Figure 3 compares the PHENIX results to data taken at different collision energies and species by plotting the relative modification of ψ' to J/ψ production ($R_{dAu}^{\psi'}/R_{dAu}^{\text{incl } J/\psi}$) as a function of charged particle multiplicity. When taking the ψ' to J/ψ ratio, a number of

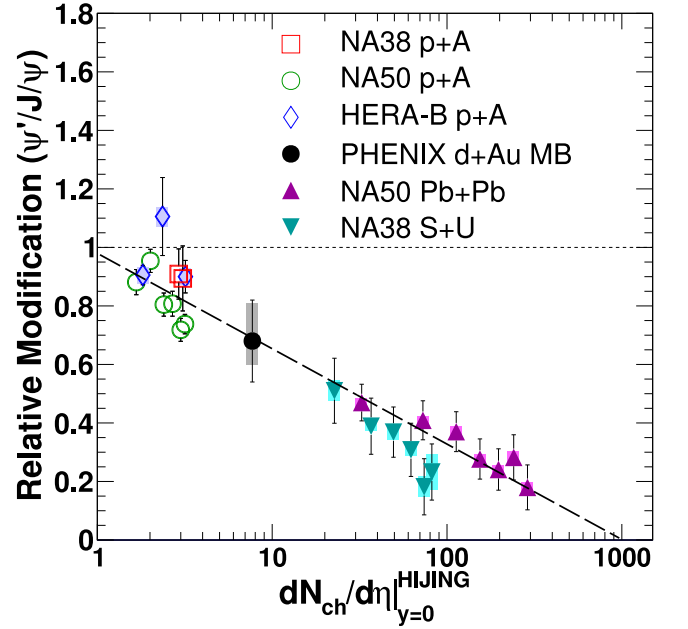


FIG. 3: (Color online) The relative modification of the ψ' to the J/ψ as a function of $dN_{ch}/d\eta|_{y=0}$. The plotted data include (open [red] squares) NA38 [2] $p+A$ at $\sqrt{s_{NN}} = 19.4$ GeV, (open [green] circles) NA50 [16] $p+A$ at $\sqrt{s_{NN}} = 27.4$ GeV, (open [blue] diamonds) HERA-B [17] $p+A$ at $\sqrt{s_{NN}} = 41.5$ with a global uncertainty of $\pm 4.4\%$, (closed [black] circles) PHENIX $d+Au$ at $\sqrt{s_{NN}} = 200$ GeV with a global uncertainty of $\pm 24\%$, (closed [magenta] upward-pointing triangle) NA50 [18] $Pb+Pb$ at $\sqrt{s_{NN}} = 17.2$ GeV, and (closed [cyan] downward-pointing triangles) NA38 [18] $S+U$ at $\sqrt{s_{NN}} = 19.4$ GeV. The SPS and HERA-B results are calculated using the extrapolated $p+p$ ψ' to J/ψ ratios quoted in the respective references. There is a common global uncertainty in the SPS points of 5% due to the uncertainty in the $p+p$ $\psi'/J/\psi$ ratio. The dashed line is included only to guide the eye.

uncertainties cancel or are reduced, such as the uncertainty in ϵA . Nuclear effects that are common between the J/ψ and ψ' (such as nuclear shadowing) will also cancel. As there are currently no measurements available of $dN_{ch}/d\eta|_{y=0}$ for the majority of the data shown in Fig. 3, we use HIJING [15] to calculate the $dN_{ch}/d\eta|_{y=0}$ values for all points. The consistent trend of results at the Super Proton Synchrotron (SPS), Hadron-Electron Ring Accelerator (HERA), and RHIC, suggests that interactions with final-state hadrons may play a role. The ψ' R_{dAu} is further calculated for different centrality bins matched to those used in the previous J/ψ analyses [5, 6].

Figure 4 shows ψ' R_{dAu} as a function of N_{coll} and also shows the previously published J/ψ R_{dAu} [5], here integrated over the full rapidity coverage of the central arm. We observe a strong suppression of ψ' production with increasing N_{coll} . The observed suppression in central $d+Au$ collisions (large N_{coll}) is a factor of ≈ 3 times larger than the observed suppression for inclusive J/ψ production.

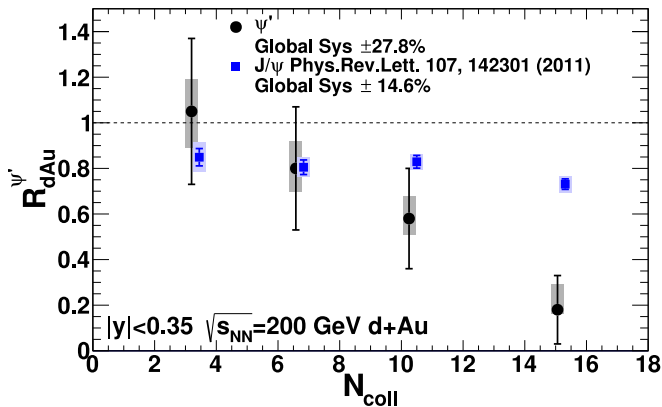


FIG. 4: (Color online) The ψ' nuclear modification factor, R_{dAu} , as a function of N_{coll} . Also included are the previously measured J/ψ R_{dAu} as a function of N_{coll} [5]. Note that the J/ψ R_{dAu} plotted here is not corrected for ψ' and χ_c feed-down, and the N_{coll} values are shifted slightly to aid in clarity.

Ref. [3] presents a model that explains the lower energy E866/NuSea and NA50 results using an expanding color neutral $c\bar{c}$ pair. As the $c\bar{c}$ expands, it has an increased nuclear absorption due to its larger physical size. Once the time spent by the $c\bar{c}$ pair traversing the nucleus becomes larger than the J/ψ formation time, the ψ' will see a larger nuclear absorption due to its larger size ($r_0 \approx 0.9$ fm for the ψ' and $r_0 \approx 0.5$ fm for the J/ψ [4]). This explains the transition from a similar level of suppression between the J/ψ and ψ' at high x_F to a larger suppression of the ψ' relative to the J/ψ at $x_F \approx 0$ observed by E866/NuSea.

This idea is tested at RHIC energies by calculating the average proper time, τ , spent in the nucleus by the quarkonia (or $c\bar{c}$ precursor). This is calculated as $\tau = \beta \langle L \rangle$, where $\langle L \rangle$ is the mean thickness of the target nucleus, and β is the average velocity of the quarkonia in the rest frame of the target nucleus. Here the J/ψ p_T is neglected. The $\langle L \rangle$ values for each centrality bin are calculated as the average center to edge distance using the same Glauber Monte Carlo model used to determine N_{coll} .

Figure 5 shows the relative modification of the ψ' to the J/ψ as a function of τ , where the E866/NuSea and NA50 results have also been included. The solid curve is the calculation by Arleo *et al.* [3], which is consistent with the trends observed by E866/NuSea and NA50.

The values of τ for the PHENIX data are similar to the $c\bar{c}$ formation and color neutralization time of ≈ 0.05 fm/c, and well below the J/ψ formation time of ≈ 0.15 fm/c [3]. Therefore the model cannot explain the strong differential suppression of the ψ' in the PHENIX data. We note that Ref. [19] shows that the extracted break up cross section for the inclusive J/ψ displays a strong departure of the E866/NuSea result from τ scaling below

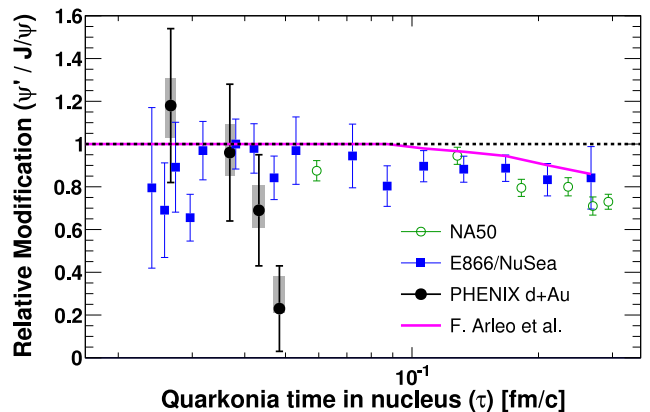


FIG. 5: (Color online) The relative modification of the ψ' to the J/ψ as a function of the proper time spent by the quarkonia (or $c\bar{c}$ precursor) in the nucleus. The data include (open [green] circles) NA50 [16] $p+A$ at 400 GeV/nucleon, (closed [blue] squares) E866/NuSea [1] $p+A$ at 800 GeV/nucleon and (closed [black] circles) PHENIX $d+Au$ at $\sqrt{s_{NN}} = 200$ GeV which include a global systematic uncertainty of $\pm 24\%$. The E866/NuSea points are calculated for ψ' and J/ψ modifications in similar rapidity intervals. The curve is a calculation by Arleo *et al.* [3] discussed in the text.

≈ 0.05 fm/c, indicating the presence of different effects that modify charmonium production at short time scales. The PHENIX data further indicate that there are effects at short crossing time scales that can differentially suppress the ψ' relative to the J/ψ .

In summary, we have presented measurements of ψ' production, as well as the J/ψ feed-down fraction from χ_c decays, in $d+Au$ collisions at $\sqrt{s_{NN}} = 200$ GeV. Using the corresponding measurements in $p+p$ collisions, we have obtained the nuclear modification factor, R_{dAu} , for ψ' and χ_c production. We find that the relative modification of ψ' to inclusive J/ψ measured by PHENIX follows the same approximate scaling with the charged particle multiplicity measured at midrapidity as lower energy data. We further find that ψ' production is heavily suppressed in central $d+Au$ collisions relative to J/ψ production. Because the nuclear crossing time is very short, this cannot be explained by the difference in size of the fully-formed ψ' and J/ψ . It instead suggests that there is a process occurring on the time scale of $c\bar{c}$ formation that differentially suppresses the ψ' .

We thank the staff of the Collider-Accelerator and Physics Departments at Brookhaven National Laboratory and the staff of the other PHENIX participating institutions for their vital contributions. We acknowledge support from the Office of Nuclear Physics in the Office of Science of the Department of Energy, the National Science Foundation, Abilene Christian University Research Council, Research Foundation of SUNY, and Dean of the College of Arts and Sciences, Vanderbilt University (U.S.A), Ministry of Education, Culture, Sports,

Science, and Technology and the Japan Society for the Promotion of Science (Japan), Conselho Nacional de Desenvolvimento Científico e Tecnológico and Fundação de Amparo à Pesquisa do Estado de São Paulo (Brazil), Natural Science Foundation of China (P. R. China), Ministry of Education, Youth and Sports (Czech Republic), Centre National de la Recherche Scientifique, Commissariat à l'Énergie Atomique, and Institut National de Physique Nucléaire et de Physique des Particules (France), Bundesministerium für Bildung und Forschung, Deutscher Akademischer Austausch Dienst, and Alexander von Humboldt Stiftung (Germany), Hungarian National Science Fund, OTKA (Hungary), Department of Atomic Energy and Department of Science and Technology (India), Israel Science Foundation (Israel), National Research Foundation and WCU program of the Ministry Education Science and Technology (Korea), Ministry of Education and Science, Russian Academy of Sciences, Federal Agency of Atomic Energy (Russia), VR and Wallenberg Foundation (Sweden), the U.S. Civilian Research and Development Foundation for the Independent States of the Former Soviet Union, the US-Hungarian Fulbright Foundation for Educational Exchange, and the US-Israel Binational Science Foundation.

* Deceased

† PHENIX Co-Spokesperson: morrison@bnl.gov

‡ PHENIX Co-Spokesperson: jamie.nagle@colorado.edu

[1] M. J. Leitch et al. (FNAL E866/NuSea Collaboration),

Phys. Rev. Lett. **84**, 3256 (2000).

[2] B. Alessandro et al. (NA50 Collaboration), Eur. Phys. J. C **48**, 329 (2006).

[3] F. Arleo, P. Gossiaux, T. Gousset, and J. Aichelin, Phys. Rev. C **61**, 054906 (2000).

[4] H. Satz, J. Phys. G **32**, R25 (2006).

[5] A. Adare et al. (PHENIX Collaboration), Phys. Rev. Lett. **107**, 142301 (2011).

[6] A. Adare et al. (PHENIX Collaboration), Phys. Rev. C **87**, 034904 (2013).

[7] A. Adare et al. (PHENIX Collaboration), Phys. Rev. D **85**, 092004 (2012).

[8] K. Adcox et al. (PHENIX Collaboration), Nucl. Instrum. Methods A **499**, 469 (2003).

[9] S. N. White, AIP Conf. Proc. **792**, 527 (2005).

[10] A. Spiridonov, arxiv:hep-ex/0510076 (2005).

[11] T. Sjostrand, S. Mrenna, and P. Z. Skands, JHEP **05**, 026 (2006).

[12] S. Frixione, P. Nason, and B. R. Webber, JHEP **0308**, 007 (2003).

[13] I. Helenius, K. J. Eskola, H. Honkanen, and C. A. Salgado, JHEP **1207**, 073 (2012).

[14] M. Cacciari, P. Nason, and R. Vogt, Phys. Rev. Lett. **95**, 122001 (2005).

[15] M. Gyulassy and X.-N. Wang, Comput. Phys. Commun. **83**, 307 (1994).

[16] M. Abreu et al. (NA38 Collaboration), Phys. Lett. B **449**, 128 (1999).

[17] I. Abt et al. (HERA-B Collaboration), Eur. Phys. J. C **49**, 545 (2007).

[18] B. Alessandro et al. (NA50 Collaboration), Eur. Phys. J. C **49**, 559 (2007).

[19] D. McGlinchey, A. Frawley, and R. Vogt, arXiv:1208.2667 (2012).